Polymer crystallization/melting induced thermal switching in a series of holographically patterned Bragg reflectors

Christopher Y. Li,*[a] Michael J. Birnkrant,[a] Lalgudi V. Natarajan,[b] Vincent P. Tondiglia,[b] Pamela F. Lloyd,[c] Richard L. Sutherland[b] and Timothy J. Bunning*[d]

Received 17th May 2005, Accepted 27th June 2005
First published as an Advance Article on the web 11th July 2005
DOI: 10.1039/b506876b

Holographic photopolymerization (H-P) is a simple, fast and attractive means to fabricate one-, two- and three-dimensional complex structures. Liquid crystals, nanoparticles and silicate nano-plates have been patterned into submicron periodical structures. In this article, we report fabrication of a one-dimensional reflection grating structure by patterning a semicrystalline polymer, polyethylene glycol (PEG), in Norland resin (thiol-ene based UV curable resin) matrix using the H-P technique. Sharp notches observed in the reflection grating of this Norland/PEG system indicate a finite Δn present in the system due to spatial segregation of the PEG and Norland resin. The notch position red shifts upon heating and the diffraction efficiency (ratio between diffraction and incident light intensity, DE) increases from $\sim$20% to 60% for the Norland 65/PEG 4600 grating. This dynamic behavior of the reflection grating is also fully reversible. The unique thermal switching behavior is attributed to the melting/formation of PEG crystals during heating/cooling. By employing different molecular weight PEGs which have different melting temperatures, a series of switching temperatures have been achieved. Since PEG can be easily coupled with a variety of functional groups, this research might shed light on fabricating multifunctional Bragg gratings using the H-P technique.

Introduction

Manufacturing dynamically controllable, multifunctional photonic structures is of crucial importance for applications such as optical elements as well as waveguides in order to control the flow of light.[1] A number of different methods, including colloid crystal assembly[2,3] and block copolymer self-assembly,[4] have been used to fabricate wavelength scale photonic structures. Shortcomings of these techniques are that lengthy sample preparation is required and defects often occur in the final products. On the other hand, holographic photopolymerization (H-P) is a simple, fast and attractive means to fabricate one-, two- and three-dimensional complex photonic structures.[5] During the H-P process, a photopolymerizable syrup is exposed to two or more coherent laser beams, interference of which creates a standing wave pattern. Higher intensity regions within the standing wave result in a locally faster polymerization process and reaction rate anisotropy, which, in turn, leads to a spatial distribution of high molecular weight polymers. Pure polymer films with a periodic refractive index (RI) modulation normal to the film surface (reflection geometry) were first fabricated several decades ago and these subsequently formed the commercial basis for DuPont's holographic component product line.[6–8] This unique technique was extended in the mid-1990s by including low molar mass, anisotropic liquid crystals (LCs) in the monomer syrup. Non-reactive LCs, normally $\sim$20–30% (w/w) of the syrup, are mixed with photopolymerizable monomers, initiators and surfactants. H-P of this mixture leads to periodically patterned, nanoscale LC droplets, a structure known as holographic polymer-dispersed liquid crystals (HPDLC).[5] The uniqueness of these structures arises from the ability to modulate the RI contrast using externally applied electric fields. This has given rise to a number of transmissive and reflective diffraction structures whose diffraction efficiency can be modulated. These unique HPDLC structures are considered one of the most attractive holographic optical elements (HOEs).[5,9] Novel three-dimensional photonic crystal structures have also been achieved by using a multiple-beam set up.[10–13]

Due to the fast kinetics of photopolymerization, these holographic structures can be fabricated within seconds and the symmetry, dimensionality, size and RI modulation can be easily controlled by the fabrication conditions. In addition to patterning LCs, Vaia *et al.* recently also applied this technique to pattern a variety of nano-sized objects.[14] By replacing the LC with gold nanoparticles (5 nm in diameter), polystyrene (PS) latex spheres (260 nm diameter) or silicate nano-plates, H-P led to one-dimensionally ordered structures with appreciable diffraction efficiency. This previous work motivated us to consider replacing either the LC or the nano-sized object with a semicrystalline polymer. Polymeric materials can be easily coupled with a variety of functional groups that are sensitive to thermal, electrical or magnetic stimulation; being able to

[a]*A. J. Drexel Nanotechnology Institute and Department of Materials Science and Engineering, Drexel University, Philadelphia, PA 19104, USA. E-mail: Chrisli@drexel.edu*
[b]*Science Applications International Corporation, 4031 Colonel Glenn Highway, Dayton, OH 45431, USA*
[c]*UES, Inc., 4401 Dayton-Xenia Rd., Dayton, OH 45432, USA*
[d]*Materials & Manufacturing Directorate, Wright-Patterson Air Force Base, OH 45433, USA. E-mail: Timothy.Bunning@wpafb.af.mil*

pattern these materials will lead to a platform for incorporating multifunctionality into the unique Bragg gratings created by the H-P technique. The resulting functional grating could thus be used for a variety of applications ranging from sensors to optical devices. In this article, we report the fabrication of Bragg reflection gratings consisting of poly(ethylene glycol) (PEG) and thiol-ene based polymers. Using the H-P technique, linear PEG was patterned into uniform one-dimensional layered structures and, due to the RI modulation between the PEG and thiol-ene polymer, Bragg reflection gratings with modest diffraction efficiencies (DE, 30–60%) were achieved. Furthermore, these PEG-based Bragg gratings possess interesting dynamic behavior triggered by thermal stimulation: a red shift of the transmission spectrum coupled with an increase of the DE upon heating is observed, presumably due to the melting of PEG crystals. The process is reversible on cooling and can be cycled numerous times. Our work represents the first example of using polymer crystal melting to modulate Bragg grating properties and it provides a generic method to achieve thermally stimulated Bragg grating modulation. Furthermore, by coupling PEG with functional groups, a variety of functional Bragg gratings can be achieved.

Experimental

Materials

The photocrosslinkable monomers used in this research are Norland optical adhesives (consisting of thiol-ene photocrosslinkable monomers) purchased from Norland Company. DAROCUR® 4265 from CIBA-GEIGY Company was used as the UV initiator. Thin sample cells were made using 8–15 μm spacers. The pre-polymer formulation consisted of Norland adhesives NOA 65 and 10–30% (w/w) PEG molecules with 3% DAROCUR® 4265 initiator. PEG with molecular weight ranging from 600 g mol^{-1} to 8000 g mol^{-1} were purchased from Aldrich and used as received.

Bragg grating writing

Writing of the grating was conducted using a Coherent Ar-ion laser (model 308C) with a laser wavelength of 363.8 nm and an output power of ~450 mW using a single beam configuration. The grating was formed as a result of interference between the incident beam and its own total internal reflection using an isosceles 90° glass prism. The cell was placed in optical contact with the prism hypotenuse using an index-matching fluid. The exposure time was typically 60 s. The prism and the cell assembly were placed on a rotation stage so that the notch wavelength could be changed easily. Faster polymerization of the monomer in the higher intensity layers led to phase separation of PEG and Norland polymers and layered structures were formed, as discussed in the following section.

Instrumentation

Bright-field transmission electron microscopy (BFTEM) was performed on a FEI CM200FEG TEM. Ultramicrotomy was performed at room temperature with an RMC PowerTome XL ultramicrotome utilizing a DiATOME 35° diamond knife. Thin (60 nm) sections of the sample were cut and floated on the water surface and subsequently collected on a TEM copper grid. Optical characterization of the reflection gratings was carried out using an Ocean Optics fiber spectrometer. A white light source coupled to a fiber-optic delivery system was used as the light source. DSC experiments were performed using a Mettler Toledo DSC822e/400 equipped with an inner liquid nitrogen cooler. Approximately 1.5 mg sample was peeled from the holographic cell and transferred to an Al DSC pan for heating and cooling tests.

Results and discussion

Bragg grating from the Norland/PEG system

As discussed in the Experimental section, reflection gratings of PEG with crosslinkable thiol-ene adhesives were fabricated using a syrup of 70% (w/w) Norland 65, 27% (w/w) of PEG and 3% (w/w) of photo-initiator.[15] Fig. 1 shows the transmission spectra of Norland 65 adhesive with 27% PEG. Four different molecular weights of PEG were used, namely, 600, 1000, 4600, and 8000 g mol^{-1}. Sharp notches are evident for all the Norland/PEG systems tested as shown below. The DE of PEG 600 and PEG 1000 samples are approximately 40–50% while those of the PEG 4600 and 8000 systems are ~20–40%. The sharp notches in the transmission spectra of these Norland/PEG systems suggest that an appreciable RI modulation has been achieved. Morphology of a Norland 65/PEG 4600 reflection grating was studied using transmission electron microscopy (TEM). Thin sections (~60 nm) of the refection grating were obtained by ultramicrotoming sample films along the film normal direction. Fig. 2a shows a TEM micrograph of a thin section of the reflection grating of the Norland 65/PEG 4600. It is evident that a long-range, uniform layered structure

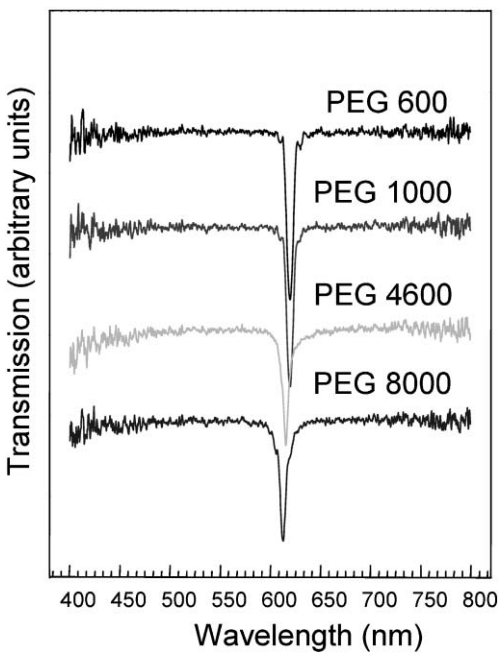

Fig. 1 Transmission spectra of the reflection gratings of PEG and Norland 65 adhesives. The baselines have been offset for clarity in display of the spectra.

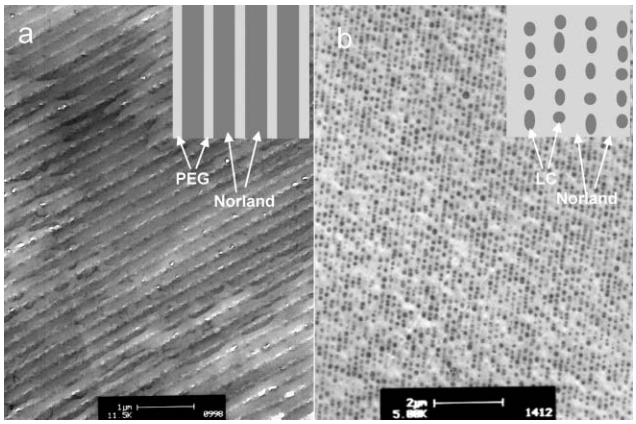

Fig. 2 (a) TEM micrograph of a thin section of a Norland 65/PEG 4600 reflection grating. White layers represent the PEG while dark areas are Norland polymers. Inset shows the schematic representation of the Norland/PEG layered structure. (b) TEM micrograph of a thin section of a Norland 65/LC(BL-38) reflection grating. Dark dots are LC droplets. Inset shows the schematic representation of the Norland/LC layered structure. Note that in b, nanoscale droplets are formed.

with alternating dark and light regions has been achieved. The dark regions represent Norland resin while the light regions represent the PEG. This assignment can be confirmed by the appearance of the "holes" in the PEG region, which results from the dissolution of PEG by water during the sample preparation process (see Experimental section). Since the RI of the polymerized Norland 65 and PEG are $\sim$1.52 and 1.4563 (or higher), respectively,[16,17] alternating PEG and Norland layers on the submicron level leads to the observation of Bragg reflection as observed in Fig. 1. Of interest is that, unlike the HPDLC systems, in which that LCs form *droplets* of 100–200 nm in diameter confined in the polymer matrix (Fig. 2b), the PEG forms a semi-continuous layer structure. This uniform layer structure could be of great interest for HPDLC device applications. All the spectra in Fig. 1 show a nearly 100% transmission light intensity of the baseline in the entire wavelength range (400–800 nm) of the spectra, which is consistent with the absence of the nanodroplets and formation of a uniform layered system as observed in the TEM experiment.

Using Fig. 2, the grating *d*-spacing was measured to be $\sim$220 nm. Since the optical properties of the patterned films can be attributed to the equation:

$$\lambda_0 \approx 2n_0\Lambda_0 \quad (1)$$

where λ_0 is the position of the notch and $n_0 \approx (0.7n_{\text{Norland}} + 0.3n_{\text{PEG}})$ is the average RI of the thiol-ene polymer and PEG. Based on the notch position of Fig. 1 and the average refractive indices of Norland 65 and PEG, the resulting grating Λ_0 can be calculated to be $\sim$208 nm, which is consistent with the TEM results.

Thermal tunability of the Norland/PEG Bragg gratings

More intriguing is that these PEG-based gratings possess dynamic behavior with respect to thermal stimulation. To demonstrate the response of the grating to temperature, the sample cells were heated from 25 °C to 70 °C at 10 °C min^{-1} followed by cooling to 25 °C at the same rate. Fig. 3 shows the *in-situ* transmission spectra of a Norland 65/PEG 4600 system at different temperatures and Fig. 4 is the plots of the DE and notch positions of Fig. 3 with respect to temperature. Upon

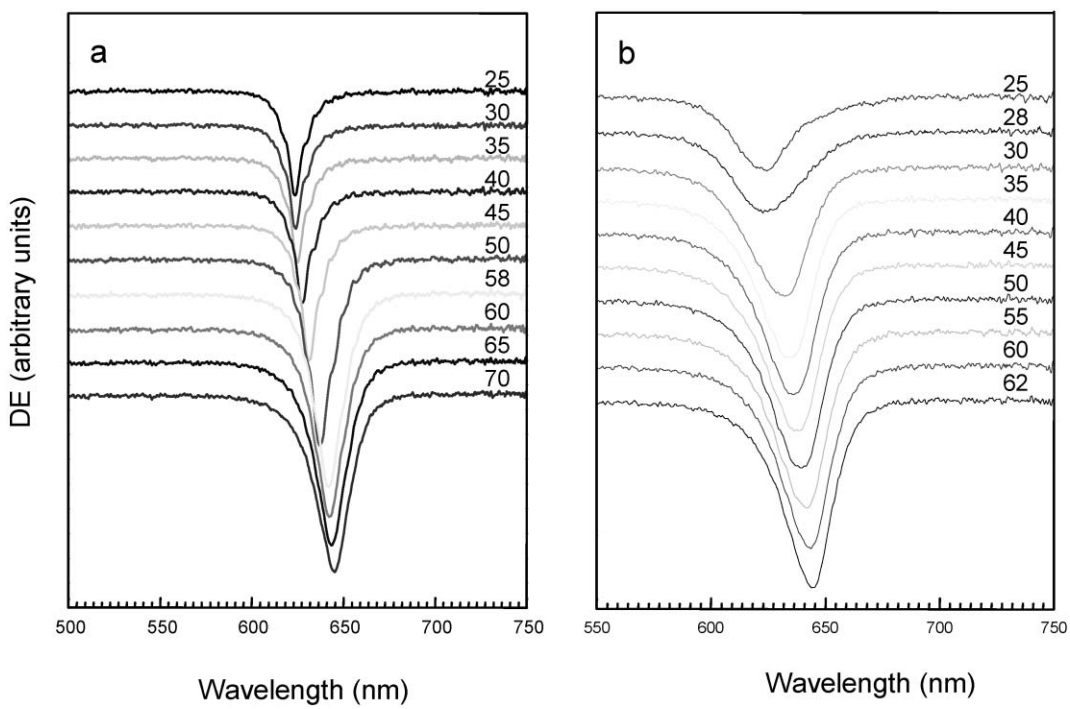

Fig. 3 Heating (a) and cooling (b) transmission spectra of a Norland 65/PEG 4600 reflection grating. The numbers on the right side of both (a) and (b) correspond to the temperatures in Celsius at which the spectra were taken.

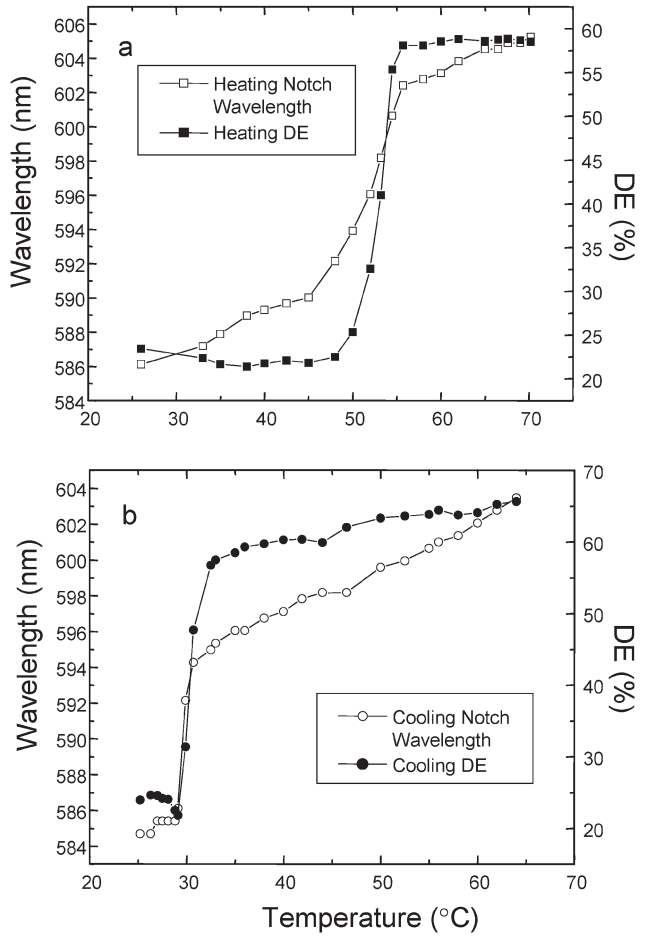

Fig. 4 Notch position and DE change with respect to temperature for Fig. 3: (a) represents heating and (b) represents cooling.

heating, the notch position red-shifts from 586 to 604 nm, and the DE increases with temperature from 20% to 60%. Upon cooling, the notch position shifts back to the original 586 nm position and the DE changes back to ~20%. In Fig. 4, there is a rapid change of DE and notch position at ~50 °C for heating and at ~30 °C for cooling. For both heating and cooling curves, the changes of DE and notch position are synchronized. A temperature tunable Bragg grating therefore has been achieved.

This unique temperature-induced notch wavelength/DE change can be attributed to the phase transition of PEG from crystalline to molten state. PEG is a semicrystalline polymer with a crystal melting point ~5–68 °C, depending upon the molecular weight.[18,19] DSC thermograms of pure PEG 4600 and the reflection grating formed by PEG 4600 reveal melting temperatures of 62 °C and 50 °C and crystallization temperatures of PEG are 38 °C and 32 °C, respectively, as shown in Fig. 5. The observation of the melting point/crystallization temperature depression in the Norland/PEG grating supports the previous work on confined polymer crystallization which suggests melting points/crystallization temperature of polymer crystals decrease in the confined state.[20,21] Of interest is that the melting and crystallization temperatures of PEG grating match well with the rapid changes of DE and notch position in

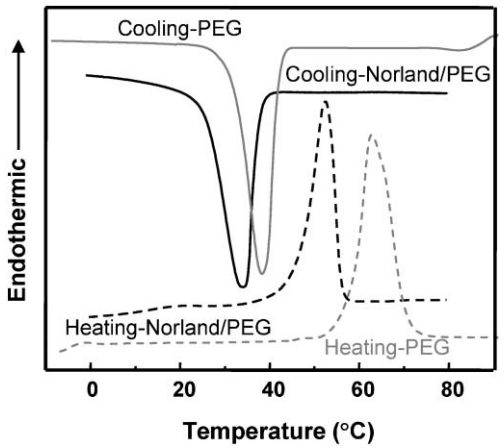

Fig. 5 DSC thermograms of pure PEG and Norland 65/PEG 4600 reflection gratings. The cooling and heating rates were controlled to be 10 °C min^{-1}.

Fig. 4, suggesting that the dynamic behavior of the PEG reflection grating is due to the crystallization/melting of the PEG crystals.

It has been recognized that both density and RI of amorphous and crystalline PEG are different. The PEG crystalline density (ρ_c) is 1.227 g cm^{-3} while the amorphous PEG density is dependent upon the temperature and it follows the following equation:

$$\rho_a = 1.1422 - 0.0008T \quad (2)$$

where T is the temperature. The ρ_a values of PEG at 30 °C and 60 °C can therefore be estimated as 1.1182 g cm^{-3} and 1.0942 g cm^{-3}, respectively.[16] PEG possesses a RI of 1.4563 (or higher at 30 °C).[17] Due to the large volume expansion during melting, the RI of the PEG crystal decreases upon melting (1.4535 at 75 °C), leading to an increase in the RI contrast between the PEG and Norland layers. This is possibly the main reason for the observation of the DE increase/decrease during melting/crystallization. Since the RI of PEG decreases upon melting, it should lead to blue shift of the notch position (according to eqn. (1), the blue shift due to the RI decrease is <2 nm, which is negligible compared to the observed 18 nm red shift), the observed red shift must be induced by an expansion of the grating. To confirm this, a quick calculation from eqn. (1) suggests that, for the given RI of the polymers, a red shift from 586 nm to 604 nm requires a ~3% expansion of the grating spacing. According to the densities of pure crystalline and amorphous PEG, ~12% volume expansion occurs upon PEG melting. However, in the PEG-based Bragg grating, not all the PEG molecules are in the crystalline form at room temperature. Crystallinity of the PEG in the grating can be calculated from the DSC results shown in Fig. 5, 100% crystalline PEG gives rise to a heat of fusion of 8.66 kJ mol^{-1},[18] whereas the heat of fusion for the PEG grating at 50 °C is ~6.93 kJ mol^{-1}. Crystallinity of PEG 4600 confined within Norland layers can therefore be calculated to be approximately 80%, which leads to 11% volume expansion of the PEG layer of the reflection grating. Assuming that the

surface area of each layer of PEG remains the same upon melting, the volume increase should solely be caused by the grating spacing expansion. Since PEG occupies ~30% of the film, the spacing of the grating should increase ~3.3% upon heating. This result matches remarkably well with the calculation of the grating expansion (3%) from the red shift of the spectra according to eqn. (1). Therefore, we can conclude that the main reason for the DE and notch position changes of the PEG-based reflection grating is the volume change driving melting/crystallization process of the PEG.

This unique dynamic behavior might find applications in sensors and thermal switching devices, *etc*. Note that the melting temperature of PEG depends upon the PEG molecular weight, suggesting that we might be able to tune the switching temperature using different molecular weight PEGs. The thermal switching behavior of PEG 8000 and PEG 2000/Norland 65 systems have been investigated and the switching temperatures during heating are 58 °C and 46 °C for PEG 8000 and PEG 2000, respectively. Both match well with the melting temperature of the PEG crystals in the confined state.

Conclusions

In conclusion, PEG has been patterned into one-dimensional sub-micron structures using the H-P technique and Norland/PEG reflection gratings were fabricated. Uniform PEG layers were observed in the grating structures with a nearly 100% background transmission in the 400–800 nm wavelength range. Sharp notches observed in the reflection grating of this Norland/PEG system indicate a finite Δn present in the system due to spatial segregation of the PEG and Norland resin. The notch position red shifts upon heating and the DE increases from ~20% to 60% for the Norland 65/PEG 4600 grating. This dynamic behavior of the reflection grating is also fully reversible. Thermal switching therefore can be realized. The unique thermal switching behavior is attributed to the melting/formation of PEG crystals during heating/cooling. By employing different molecular weight PEGs which have different melting temperatures, a series of switching temperatures have been achieved. Since PEG can be easily coupled with a variety of functional groups, this research might shed light on fabricating multifunctional Bragg gratings using the H-P technique. Due to the biocompatibility of PEG, the present research also suggests that patterning biomolecules using holographic polymerization might also be possible by employing PEG as the carrying vehicle.

Acknowledgements

This work is supported by the NRC/US AFOSR Summer Faculty Fellowship and NSF CAREER award (DMR-0239415). CYL thanks the Mettler-Toledo Co. for the Turi award supporting the thermal analysis equipment purchase. MJB thanks the NSF IGERT fellowship (DGE-0221664) for support.

References

1 J. D. Joannopoulos, P. R. Villeneuve and S. H. Fan, *Nature*, 1997, **386**, 143–149.
2 Y. N. Xia, B. Gates, Y. D. Yin and Y. Lu, *Adv. Mater.*, 2000, **12**, 693–713.
3 S. H. Foulger, S. Kotha, B. Seryda-Krawiec, T. W. Baughman, J. M. Ballato, P. Jiang and D. W. Smith, Jr., *Opt. Lett.*, 2000, **25**, 1300–1302.
4 Y. Fink, A. M. Urbas, M. G. Bawendi, J. D. Joannopoulos and E. L. Thomas, *J. Lightwave Technol.*, 1999, **17**, 1963–1969.
5 T. J. Bunning, L. V. Natarajan, V. P. Tondiglia and R. L. Sutherland, *Annu. Rev. Mater. Sci.*, 2000, **30**, 83–115.
6 W. S. Colburn and K. A. Haines, *Appl. Opt.*, 1971, **10**, 1636–1641.
7 W. J. Gambogi, A. M. Weber and T. J. Trout, *SPIE Proc.*, 1994, **2043**, 2–13.
8 W. K. Smothers, B. M. Moroe, A. M. Weber and D. E. Keys, *SPIE Proc.*, 1990, **1212**, 20–29.
9 R. L. Sutherland, V. P. Tondiglia, L. V. Natarajan and T. J. Bunning, *J. App. Phys.*, 2004, **96**, 2, 951–965.
10 V. P. Tondiglia, L. V. Natarajan, R. L. Sutherland, D. Tomlin and T. J. Bunning, *Adv. Mater.*, 2002, **14**, 3, 187–191.
11 M. Campbell, D. N. Sharp, M. T. Harrison, R. G. Denning and A. J. Turberfield, *Nature*, 2000, **404**, 53–56.
12 R. L. Sutherland, V. P. Tondiglia, L. V. Natarajan, S. Chandra, D. Tomlin and T. J. Bunning, *Opt. Express*, 2002, **10**, 1074–1082.
13 M. J. Escuti, J. Qi and G. P. Crawford, *Opt. Lett.*, 2003, **28**, 522–524.
14 R. A. Vaia, C. L. Dennis, L. V. Natarajan, V. P. Tondiglia, D. W. Tomlin and T. J. Bunning, *Adv. Mater.*, 2001, **13**, 20, 1570–1574.
15 L. V. Natarajan, C. K. Shepherd, D. M. Brandelik, R. L. Sutherland, S. Chandra, V. P. Tondiglia, D. Tomlin and T. J. Bunning, *Chem. Mater.*, 2003, **15**, 12, 2477–2484.
16 J. Brandrup, E. H. Immergut and E. A. Grulke, *Polymer Handbook*, John Wiley, New York, 1999.
17 J. D. Ingham and D. D. Lawson, *J. Polym. Sci.*, 1965, **3**, 2707–2710.
18 B. Wunderlich, *Thermal Analysis*, Academic Press, Boston, 1990.
19 B. Wunderlich, *Macromolecular Physics*, Academic Press, Boston, 1980, vol. 3.
20 P. Huang, L. Zhu, Y. Guo, Q. Ge, A. J. Jing, W. Y. Chen, R. P. Quirk, S. Z. D. Cheng, E. L. Thomas, B. Lotz, B. S. Hsiao, C. A. Avila-Orta and I. Sics, *Macromolecules*, 2004, **37**, 3689–3698.
21 Y.-L. Loo, R. A. Register, A. J. Ryan and G. T. Dee, *Macromolecules*, 2001, **34**, 8968–8977.

